

# Lecture 2

## Wetting and Spreading

In Lecture 1, we have discussed the concept of surface tension. Increasing the surface area always raises the free energy of the system. As a consequence there is a tendency to reduce surface area. A well-known example of this phenomenon is that a suspended water droplet is always spherical when gravity is negligible (i.e. in space station or at microscopic scale). However, the situation becomes different when we consider the interface between solid / liquid phase A with a flat surface and liquid phase B. When the two phases contact, the liquid B may either (i) spreads on A, forming a thin liquid film, or (ii) partially wet B, forming a droplet (Figure 2.1).

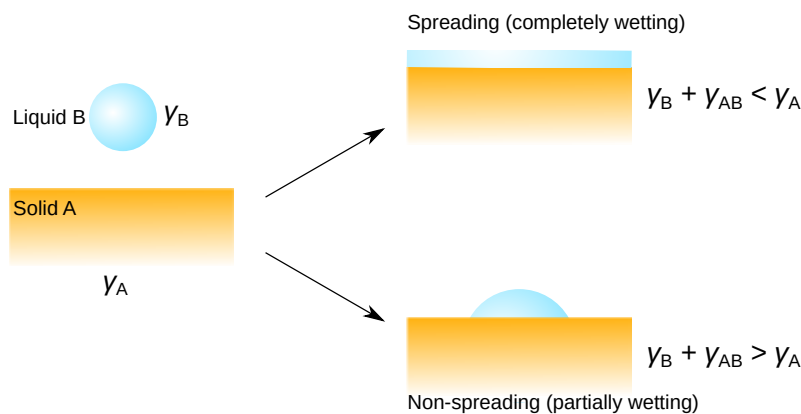


Figure 2.1: Spreading and partial wetting at the liquid-solid interface.

What factors determine the formation of a wetting layer / droplet? Can we model the shape of the droplet? In this lecture we will try to answer the above question using our knowledge of surface tension.

### 2.1 The relation between wetting and surface tension

The criteria determining whether spreading or partial wetting happens, is the relative magnitudes between  $\gamma_A$ ,  $\gamma_B$  and  $\gamma_{AB}$ . We can define a quantity “spreading coefficient”,<sup>1</sup>  $S_{B/A}$ ,

such that:

$$S_{B/A} = \gamma_A - (\gamma_B + \gamma_{AB}) \quad (2.1)$$

If  $S_{B/A} > 0$ , liquid A can completely wet B, and *vice versa*. This can happen when  $\gamma_A$  is large. As an example we can use the spreading coefficient to explain the wetting between different liquids. As shown in Table 2.1, low surface tension liquids (hexane, benzene and oleic acid) completely wet on the water surface and form films, while  $\text{CS}_2$  and  $\text{CH}_2\text{I}_2$  do not wet on water and form droplets. On the contrary, all these liquids completely wet on the surface of mercury, due to the extremely large  $\gamma$ . However, we should see that the spreading behavior cannot be simply judged from  $\gamma_A$  or  $\gamma_B$  alone: oleic acid and  $\text{CS}_2$  have almost the same surface tension, however oleic acid spreads on water while  $\text{CS}_2$  only partially wets. In other words, our simplified model for the interfacial tension  $\gamma_{AB}$  from Equation 1.11 is not sufficient to explain some real liquids.

Table 2.1: Spreading coefficient  $S_{B/A}$  for different liquids on water and mercury surface. All data are in  $\text{mJ}\cdot\text{m}^{-2}$ .

S \ B	A	Water $\gamma=72$	Mercury $\gamma=489$
	Hexane $\gamma \approx 20$		3.4
Benzene $\gamma \approx 30$		8.9	99
Oleic acid $\gamma \approx 35$		24.6	102
$\text{CS}_2$ $\gamma \approx 35$		-8.2	102
$\text{CH}_2\text{I}_2$ $\gamma \approx 50$		-26.5	70

## 2.2 The contact angle

Although the spreading coefficient  $S_{B/A}$  is useful to distinguish whether a liquid spreads on the surface, in the case of partial wetting, we still want to quantify how “well” the liquid wets. We can do this by measuring the **contact angle** of a liquid droplet (L) on a solid surface (S) in air (Figure 2.2). The contact angle is the angle between the liquid-air and liquid-

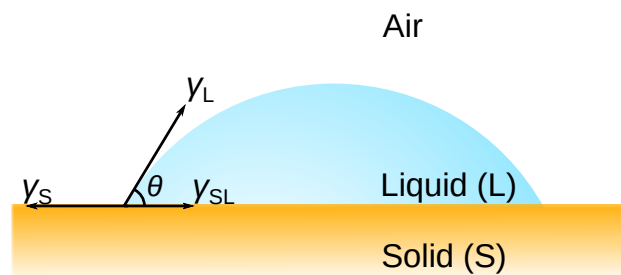


Figure 2.2: The relationship between the contact angle of a droplet  $\theta$ , and the surface tensions.

solid contact lines, and is highly related with the surface tensions. Recall in Lecture 1 the surface tension also have unit of [force]/[length], in fact, in a microscopical view, the surface tension is a force that operates along the interface contact line,<sup>2</sup> which tends to decrease the surface area. Near the triple-phase contact line of a droplet at equilibrium, there is a force balance between the surface tensions  $\gamma_L$ ,  $\gamma_S$  and  $\gamma_{SL}$ :

$$\gamma_S = \gamma_L \cos \theta + \gamma_{SL} \quad (2.2)$$

which is known as the Young equation<sup>3</sup> of contact angle. Use the relation in Equation 1.4, the Young equation can also be rewritten as:

$$\gamma_L(1 + \cos \theta_Y) = \Delta W_{SL} \quad (2.3)$$

which is also known as the Young-Dupré equation,<sup>4</sup> where  $\theta_Y$  is the static contact angle described by the Young-Dupré equation. Equation 2.3 relates two macroscopic (and easily measurable) quantities  $\theta_Y$  and  $\gamma_L$  with the work of adhesion  $\Delta W_{AB}$ . From our microscopic model in Lecture 1,  $\theta_Y$  can be written using the Hamaker constant  $A_{SL}$  and equilibrium solid-liquid interface distance  $d_{SL}$  as:

$$\theta_Y = \arccos \left[ \frac{A_{SL}}{12\pi d_{SL}^2} \frac{1}{\gamma_L} - 1 \right] \quad (2.4)$$

Since  $d_{SL}$  for almost all liquid-solid interface is usually at the order of 5 Å, the contact angle can be qualitatively inferred from  $A_{SL}$  and  $\gamma_L$ :

- Higher  $A_{SL}$ : the adhesion between S and L is strong  $\rightarrow$  smaller  $\theta_Y$  (more wetting)
- Higher  $\gamma_L$ : more energy is required for wetting  $\rightarrow$  larger  $\theta_Y$  (less wetting)

An extreme case is when  $\Delta W_{SL} = 0$ , we have  $\theta_Y=180^\circ$ , i.e. the liquid cannot wet the surface at all.

## 2.3 Measuring surface tension

As you can imagine, the surface tension of a liquid can be measured as a force acting on the boundary, using an instrument called the **tensiometer**. A widely-used design of the tensiometer is the Wilhelmy plate method, named after its inventor Ludwig Wilhelmy. A typical setup for the Wilhelmy plate can be seen in Figure 2.3, where a thin plate (S) with thickness  $d$  and width  $W$  ( $d \ll W$ ) is immersed in a liquid (L) with an immersion depth of  $H$ . The liquid forms contact angle  $\theta$  on both sides of the plate. When moving the plate in the  $z$  direction, a total force  $F_{tot}$  is measured using a micro balance, which is further converted to the surface tension  $\gamma$ .

The total force  $F_{tot} = F_{wetting} + F_{bouy} + F_{weight}$ , where  $F_{wetting}$  is the wetting force on the contact line,  $F_{bouy} = -\rho_L g dWH$  is the buoyancy force, and  $F_{weight}$  is the gravity of the plate.

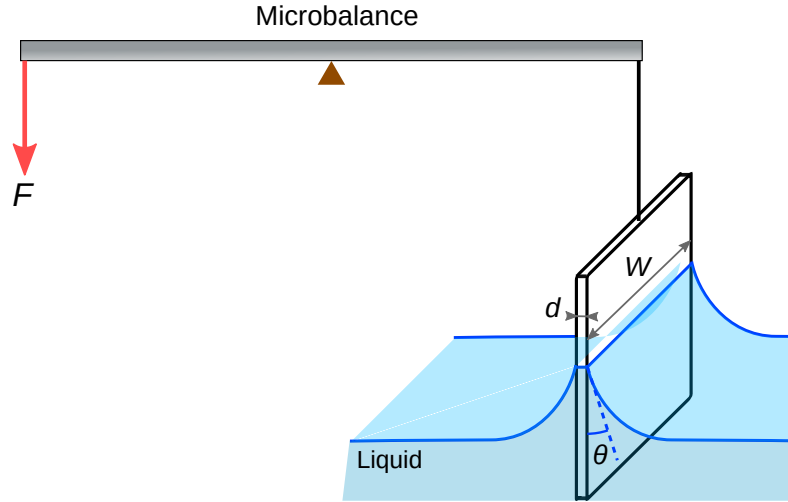


Figure 2.3: Scheme of the Wilhelmy plate used to measure the surface tension of a liquid.

Both  $F_{\text{bouy}}$  and  $F_{\text{weight}}$  can be determined using geometric parameters and are usually very small compared with  $F_{\text{wetting}}$  since  $d \ll W$ . At steady state,  $F_{\text{wetting}}$  is expressed as:

$$F_{\text{wetting}} = \gamma_L \cos \theta [2(d + W)] \approx 2W\gamma_L \cos \theta \quad (2.5)$$

If  $\theta \rightarrow 0$ , i.e. complete wetting on the plate, we can estimate the surface tension as  $\gamma_L = F_{\text{wetting}}/2W \approx F_{\text{tot}}/2W$ . However this equation does not work for larger contact angles, and should be used with care.

Besides the Wilhelmy plate method, there are many other techniques to determine the surface tension  $\gamma$ , including the capillary rise method,<sup>5</sup> pendant droplet method,<sup>6</sup> Du Nouy ring method,<sup>7</sup> etc. Each method has its advantages and limitations, and has to be chosen with care.

## 2.4 Wetting on real surfaces

The discussion about the contact angle so far has been made regarding the flat surface. A water contact angle larger than  $120^\circ$  is quite unusual for flat surfaces.<sup>8</sup> This is not hard to imagine, using the simple model that  $\gamma_{\text{SL}} = (\sqrt{\gamma_{\text{S}}} - \sqrt{\gamma_{\text{L}}})^2$ , we get  $\Delta W_{\text{SL}} = 2\sqrt{\gamma_{\text{S}}\gamma_{\text{L}}}$ . Plug it into Equation 2.3, we have:

$$\cos \theta_Y = 2\sqrt{\frac{\gamma_{\text{S}}}{\gamma_{\text{L}}}} - 1 \quad (2.6)$$

If  $\theta_Y$  is  $120^\circ$ , we need  $\gamma_{\text{S}}$  as low as  $5 \text{ mJ}\cdot\text{m}^{-2}$ , which is even much smaller than teflon. Although such analysis oversimplifies  $\gamma_{\text{SL}}$ , we can infer that a higher  $\theta_Y$  than  $120^\circ$  for water on an ideally flat surface, is merely unphysical.

However, in daily life we often observe the contact angle to be much larger than  $150^\circ$  on some plant leaves and flower pedals which have rough surfaces. Usually on a rough

surface, the macroscopic static contact angle  $\theta^*$ , is different from the static contact angle  $\theta_Y$  on a flat surface. Depending on the relative magnitudes between  $\theta^*$  and  $\theta_Y$ , there are two models to describe the wetting on a rough surface (Figure 2.4)

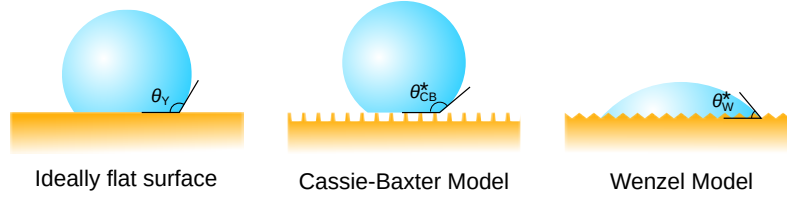


Figure 2.4: Wetting on a flat surface and on a rough surface described by Cassie-Baxter and Wenzel models.

- $\theta^* > \theta_Y$  (Cassie-Baxter model<sup>9</sup>)

In the Cassie-Baxter (CB) model, there are air voids within the rough structure on the surface that cannot be wetted, and therefore surface roughness leads to less wetting.  $\theta^*$  in the CB model is written as:

$$\cos \theta_{CB}^* = r f \cos \theta_Y + f - 1 \quad (2.7)$$

where  $r$  is the roughness factor of the surface, and  $f$  is the fraction of wetted surface area

- $\theta^* < \theta_Y$  (Wenzel model<sup>10</sup>)

In the Wenzel (W) model, the liquid can completely wet the rough structure, and leads to more wetting. The fraction  $f$  in the CB model becomes 1 and  $\theta^*$  is simply controlled by  $r$

$$\cos \theta_W^* = r \cos \theta_Y \quad (2.8)$$

In the end, we can see that both models have a similar physical background, and the Wenzel model is the special case of Cassie-Baxter model when  $f = 1$ . The different wetting phenomena lead to some interesting properties. Usually for a **hydrophobic** material with ( $\theta_Y > 90^\circ$ ), surface roughness leads to the Cassie-Baxter wetting state, and  $\theta^*$  can approach  $180^\circ$  (**superhydrophobic**). On the other hand, for a **hydrophilic** material ( $\theta \ll 90^\circ$ ), the surface roughness leads to the Wenzel wetting states and makes the surface **superhydrophilic** ( $\theta^* \rightarrow 0^\circ$ ).

On a real surface, the contact angle of a moving contact line can be different from the static contact angle  $\theta^*$ . The contact angle when the contact line advances is called the **advancing angle**  $\theta_{adv}$ , and the contact angle when the contact line shrinks is called the **receding angle**  $\theta_{rec}$  (Figure 2.5). The difference between the dynamic contact angles comes from the local defects that “pins” the contact line, and we have  $\theta_{adv} > \theta^* > \theta_{rec}$ . This phenomenon is known as the **contact angle hysteresis** and several models have been proposed to explain its origin.<sup>11-13</sup>

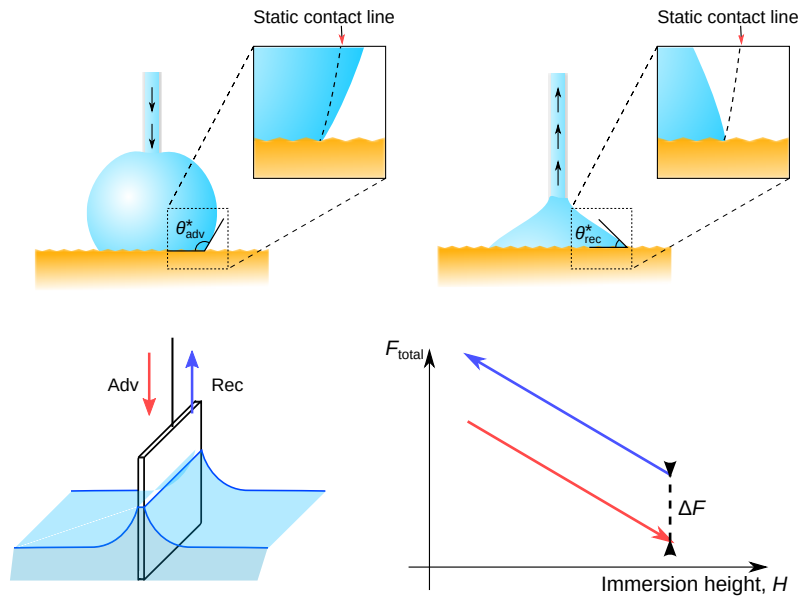


Figure 2.5: Dynamic contact angles and the measurement of contact angle hysteresis from Wilhelmy plate method.

An ideally flat surface should have contact angle hysteresis close to  $0^\circ$ . The hysteresis, defined as the difference between  $\theta_{adv}$  and  $\theta_{rec}$  is also measurable through the Wilhelmy plate method. As shown in Figure 2.5, the force curve of total force  $F_{tot}$  as a function of immersion height  $h$  do not overlap between the advancing (dipping) and receding (lifting) processes. The displacement force  $\Delta F$  between the two curves can be written using our previous knowledge as:

$$\Delta F \approx 2W\gamma_L(\cos \theta_{rec} - \cos \theta_{adv}) \quad (2.9)$$

# References

- (1) Ross, S.; Becher, P. *J. Colloid Interface Sci.* **1992**, *149*, 575–579.
- (2) Marchand, A.; Weijs, J. H.; Snoeijer, J. H.; Andreotti, B. *Am. J. Phys.* **2011**, *79*, 999–1008.
- (3) Young, T. *Phil. Trans. R. Soc. of Lond.* **1805**, *95*, 65–87.
- (4) Schrader, M. E. *Langmuir* **1995**, *11*, 3585–3589.
- (5) Richards, T. W.; Carver, E. K. *J. Am. Chem. Soc.* **1921**, *43*, 827–847.
- (6) Berry, J. D.; Neeson, M. J.; Dagastine, R. R.; Chan, D. Y.; Tabor, R. F. *J. Colloid Interface Sc.* **2015**, *454*, 226–237.
- (7) Du Nouy, P. L. *J. Gen. Physiol.* **1925**, *7*, 625–631.
- (8) Quéré, D. *Physica A* **2002**, *313*, 32–46.
- (9) Cassie, A. B. D.; Baxter, S. *Trans. Faraday Soc.* **1944**, *40*, 546.
- (10) Wenzel, R. N. *Ind. Eng. Chem.* **1936**, *28*, 988–994.
- (11) Joanny, J. F.; de Gennes, P. G. *J. Chem. Phys.* **1984**, *81*, 552–562.
- (12) Patankar, N. A. *Langmuir* **2010**, *26*, 7498–7503.
- (13) Yeh, K.-Y.; Chen, L.-J.; Chang, J.-Y. *Langmuir* **2008**, *24*, 245–251.

